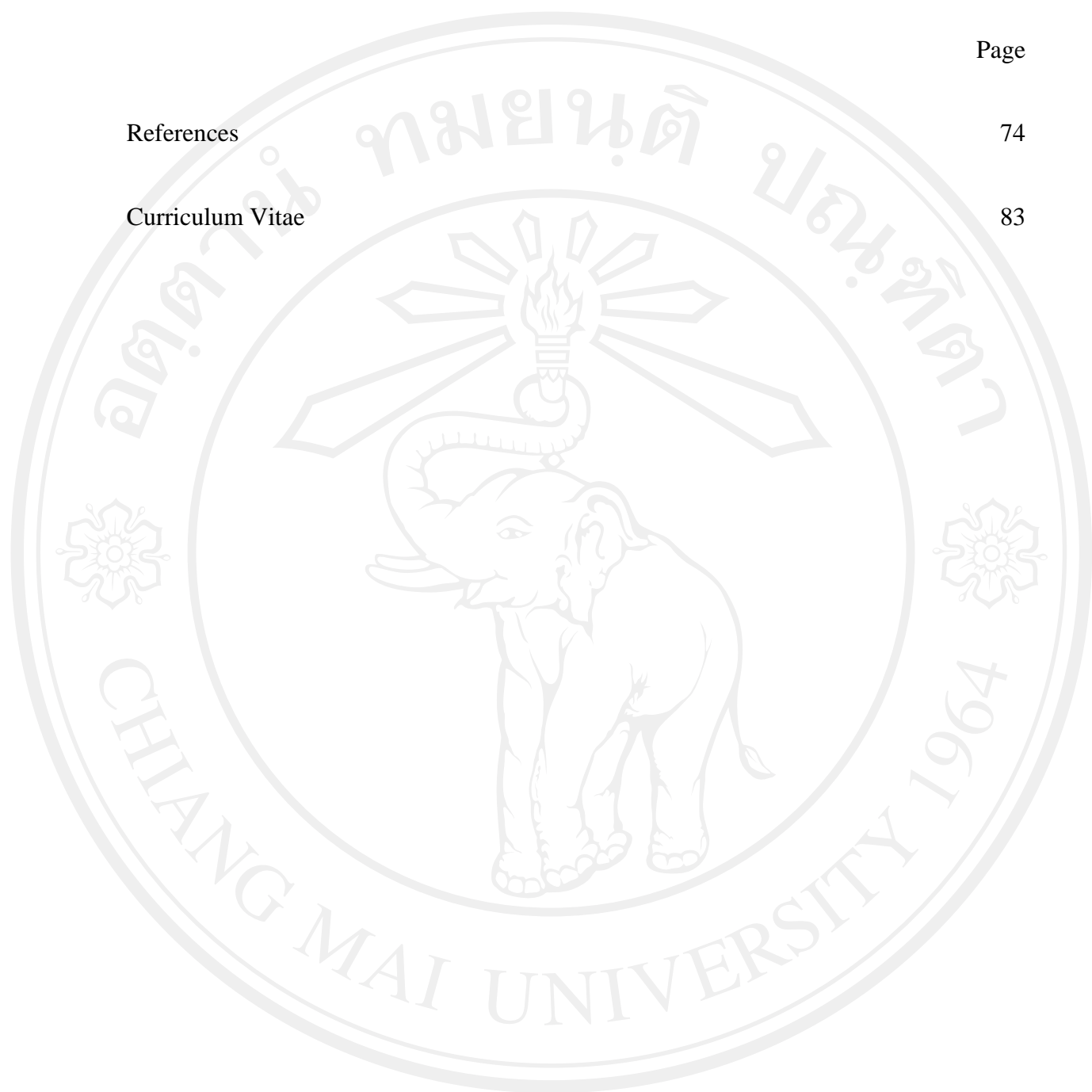


## CONTENT

	Page
Acknowledgement	c
Abstract in Thai	d
Abstract in English	e
List of Tables	i
List of Figures	k
List of Abbreviations	o
List of Symbols	p
Chapter 1 Introduction	1
1.1 Historical Background	1
1.2 Objectives	4
1.3 Scope of Study	4
1.4 Educational Application Advantages	5
Chapter 2 Literature Review	6
2.1 Dye-Sensitized Solar Cell	6
2.2 Titanium Dioxide	6

	Page
2.3 Diamond-Like Carbon	8
2.4 Filtered Cathodic Vacuum Arc Deposition	10
2.5 Annealing of the film	20
2.6 Analysis technique	21
2.7 Photovoltaic Properties Efficiency	31
2.8 Photocatalytic Antibacterial Properties	33
2.9 Mechanical Properties of DLC	33
<b>Chapter 3 Experimental Processes</b>	<b>36</b>
3.1 Substrate Preparation	36
3.2 Film Deposition	37
3.3 Analysis of the Thin Film	43
<b>Chapter 4 Results and Discussions</b>	<b>49</b>
4.1 TiO <sub>2</sub> Film Preparation	49
4.2 Application as a Solar Cell	63
4.3 Application as an Antibacterial Compound	65
4.4 DLC Film Preparation	67
<b>Chapter 5 Conclusions and Suggestions</b>	<b>71</b>
5.1 Conclusions	71
5.2 Suggestions	73

	Page
References	74
Curriculum Vitae	83



ลิขสิทธิ์มหาวิทยาลัยเชียงใหม่

Copyright© by Chiang Mai University  
All rights reserved

## LIST OF TABLES

	Page
Table 2.1 Comparison of major properties of amorphous carbons with those of reference materials diamond, graphite, C <sub>60</sub> and polyethylene	8
Table 2.2 Two types of cathodic arc sources which named by its applying current; continuous direct current (DC) and pulsed current	12
Table 2.3 An example of calculated atomic percentage	24
Table 3.1 Various substrate types for their specific analysis techniques	36
Table 3.2 The TiO <sub>2</sub> film deposited with various deposition conditions	42
Table 4.1 A summary of the deposition and characterization of the 20-min deposited TiO <sub>2</sub> film for SEM, EDS, Raman analysis and AFM	51
Table 4.2 The atomic percentage of elements in film on various O <sub>2</sub> pressures.	54
Table 4.3 The relative atomic percentage varied by varying O <sub>2</sub> pressure.	55
Table 4.4 The varied bias voltage and deposition time TiO <sub>2</sub> deposited substrate's calculated thickness and density.	57
Table 4.5 The summary of deposition condition for the annealing and deposition time effect on film experiment.	59
Table 4.6 The 6 deposition conditions of TiO <sub>2</sub> deposited FTO glass to be a part of DSSC.	63
Table 4.7 The raw data of the photocatalytic antibacterial test result.	66

Table 4.8 The several DLC deposition conditions deposited at arc voltage 600 V, 10 minutes deposition time, base pressure at  $5 \times 10^{-5}$  torr with different bias voltage. 67

Table 4.9 The several DLC deposition conditions deposited at arc voltage 600 V, -250 V biased, 10 minutes deposition time, base pressure at  $5 \times 10^{-5}$  torr with different working pressure of  $N_2$ . 68

## LIST OF FIGURES

	Page
Figure 1.1 Reported timeline of solar cell energy conversion efficiencies.	1
Figure 1.2 Dye-sensitized solar cell.	2
Figure 1.3 The Photograph of the in-house developed FCVAD system at Chiang Mai University.	3
Figure 1.4 Hard disk architecture.	4
Figure 2.1 Unit cells of 3 main phases of TiO <sub>2</sub> .	7
Figure 2.2 The various phases of diamond-like carbon.	9
Figure 2.3 Components of a DLC material.	9
Figure 2.4 Schematic of FCVAD system.	10
Figure 2.5 Ion current from different elements plotted as a function of arc current.	13
Figure 2.6 Schematic of a 1995 Berkeley Lab's miniature cathodic arc source.	15
Figure 2.7 Schematic of a SEM's installed electron gun.	21
Figure 2.8 Schematic of an arranged SEM's instruments.	22
Figure 2.9 Atomic levels involved in copper K <sub>α</sub> and K <sub>β</sub> emission.	23
Figure 2.10 The EDS spectrum of a high temperature nickel based alloy which is plotted between the spectrum's energy-count.	24
Figure 2.11 The three spectrums and their relative intensity detected after an intense laser beam emits onto a material's surface.	26
Figure 2.12 Crystal structure of anatase phase.	27
Figure 2.13 The Raman spectrum of anatase and rutile TiO <sub>2</sub> .	27
Figure 2.14 Raman spectrum is dominated by G peak and D peak of the sp <sup>2</sup> configuration, indirect method on sp <sup>3</sup> /sp <sup>2</sup> ratio.	28
Figure 2.15 The Eigen vectors of Raman sp <sup>2</sup> G and D mode respectively.	28
Figure 2.16 A laser beam is in used to provide observing the cantilever movement by the detector.	30

	Page
Figure 2.17 Different surface analysis AFM modes identified by their operating range between the AFM's tip and sample's surface.	30
Figure 2.18 Schematic of DSSC photovoltaic properties testing.	32
Figure 2.19 An example of the V-I plotted solar cell's photovoltaic properties test.	32
Figure 2.20 (red line) The current-voltage curve obtained from raw data.	33
Figure 2.21 Hysitron™ triboindenter plays a role measure the films' hardness and adhesion.	34
Figure 2.22 The specimen is dragging in the horizontal direction while the applied normal force is increasing overtime.	34
Figure 2.23 The increasing applied normal force is measured overtime to detect the critical load where the friction force increases suddenly.	35
Figure 3.1 Small pure titanium rod is attached to the end of stainless steel rod.	37
Figure 3.2 FCVAD cathode holder and substrate holder.	38
Figure 3.3 The installed instrument in a deposition chamber.	38
Figure 3.4 Active guage controller is being used to measure the deposition chamber's pressure lower than $2 \times 10^{-2}$ torr.	39
Figure 3.5 The power supply is set to provide a fixed arc voltage at 0.600 kV without fixing arc current.	39
Figure 3.6 The pulsed plasma of Ti with O <sub>2</sub> doped (a) top view (b) side view.	40
Figure 3.7 The peak of 6.10 Volts is measured.	40
Figure 3.8 The TiO <sub>2</sub> post-deposited substrates	41
Figure 3.9 The LTD® annealing furnace is being used for annealing TiO <sub>2</sub> film.	41
Figure 3.10 Gold-coated TiO <sub>2</sub> -deposited substrates attached on top and side of SEM's stubs.	43
Figure 3.11 The JEOL® JSM 6335F is being used for analyzing the film by both SEM and EDS techniques in this study.	44
Figure 3.12 Renishaw InVia Reflex Raman spectrometer	44
Figure 3.13 AFM system.	45
Figure 3.14 N719 dye solution soaked annealed TiO <sub>2</sub> coated FTO glasses.	46

	Page
Figure 3.15 Iodine half-filled after testing DSSC.	46
Figure 3.16 The power conversion efficiency test system.	47
Figure 3.17 Schematic of the power conversion efficiency experiment circuit.	47
Figure 3.18 The setup for testing TiO <sub>2</sub> film photocatalytic antibacterial effect.	48
Figure 4.1 The deposited film on varying distance 1cm and 3cm, with arc voltage 600V, bias -250V, pressure 4.2x10 <sup>-3</sup> for 20 minutes.	49
Figure 4.2 The film transparency as a function of the working pressure.	51
Figure 4.3 SEM images of the films.	52
Figure 4.4 AFM-measured film surface morphology across the boundary between the film and the substrate as a function of the working pressure.	53
Figure 4.5 The thickness of films deposited at different oxygen doping pressure.	53
Figure 4.6 An example of the EDS information of the titanium dioxide thin film which is deposited at 10 <sup>-4</sup> torr, arc 600 V and -250 V biased with 20 minutes deposition time.	54
Figure 4.7 The plotted relative atomic percentage varied by varying of O <sub>2</sub> pressure with making use of the non-doping condition as a reference.	55
Figure 4.8 The deposited TiO <sub>2</sub> film with different oxygen doping pressure at 10 <sup>-1</sup> torr, 10 <sup>-2</sup> torr, 10 <sup>-3</sup> torr and non-oxygen doped at the base pressure at 5x10 <sup>-5</sup> torr.	56
Figure 4.9 The relationship between film's mass and deposition time.	57
Figure 4.10 The relationship between film's thickness and deposition time.	58
Figure 4.11 The relationship between film's density and deposition time.	58
Figure 4.12 The not annealed TiO <sub>2</sub> film deposited with O <sub>2</sub> doped pressure at 10 <sup>-3</sup> torr for 10 minutes, 20 minutes and 30 minutes deposition time.	60
Figure 4.13 The annealed TiO <sub>2</sub> film deposited with O <sub>2</sub> doped pressure at 10 <sup>-3</sup> torr for 10 minutes, 20 minutes and 30 minutes deposition time.	61
Figure 4.14 The deposited TiO <sub>2</sub> film with different O <sub>2</sub> doped pressure 10 <sup>-3</sup> torr and 10 <sup>-2</sup> torr.	61



	Page
Figure 4.15 The deposited TiO <sub>2</sub> film with annealed and not annealed condition deposited with O <sub>2</sub> doped pressure at 10 <sup>-3</sup> torr.	62
Figure 4.16 The deposited TiO <sub>2</sub> film with annealed and not annealed condition deposited with O <sub>2</sub> doped pressure at 10 <sup>-2</sup> torr.	62
Figure 4.17 The circuit's current density affected by varying the source's voltage in annealed and non-annealed TiO <sub>2</sub> deposited FTO glasses.	64
Figure 4.18 The circuit's current density affected by varying the source's voltage in non-biased and -250 V biased TiO <sub>2</sub> deposited FTO glasses.	64
Figure 4.19 The circuit's current density affected by varying the source's voltage in 20 min and 30 min deposition time of TiO <sub>2</sub> deposited FTO glasses.	64
Figure 4.20 The Raman spectrum of DLC with varied bias voltage.	67
Figure 4.21 The plotted ratio of the intensity between D peak and G peak of the films with varied bias voltage from 0 V to -450 V.	68
Figure 4.22 The Raman spectrum of the DLC with various working pressure of N <sub>2</sub> .	69
Figure 4.23 Summarized tested properties of DLC films; Hardness, Critical load and intensity ratio between D peak and G peak.	69

## LIST OF ABBREVIATIONS

AFM	Atomic Force Microscopy
a-C:H	Hydrogen doped Amorphous Carbon
CBM	Conduction Band Minimum
DC	Direct Current
DSSC	Dye-Sensitized Solar Cell
DLC	Diamond-Like Carbon
D peak	Disorder Peak
EDS, EDX	Energy-Dispersive X-ray Spectroscopy
FCVA	Filtered Cathodic Vacuum Arc
FCVAD	Filtered Cathodic Vacuum Arc Deposition
FTO	Fluorine Doped Tin Oxide
G peak	Graphite Peak
SEM	Scanning Electron Microscopy
TCO	Transparent Conducting Glass
TiO <sub>2</sub>	Titanium Dioxide
ta-C	Tetrahedral Amorphous Carbon
ta-C:N	Nitrogen doped Tetrahedral Amorphous Carbon
UV	Ultraviolet

## LIST OF SYMBOLS

<b>A</b>	Projected Contact Area
<i>d</i>	Plasma's Duty Cycle
<b>F</b>	AFM Measured Force
<b>F<sub>max</sub></b>	Maximum Load which causes a constant penetration depth
<b>FF</b>	Fill Factor
<b>H</b>	Hardness
<b>x</b>	Cantilever Deflection
<b>J<sub>sc</sub></b>	Short Circuit Current Density
<b>J<sub>mp</sub></b>	Current Density that provides Maximum Power
<b>k</b>	Spring Constant
<b>κ</b>	System Coefficient
<b>κ<sub>eff</sub></b>	Filter Efficiency
<b>V<sub>oc</sub></b>	Open Circuit Voltage
<b>V<sub>mp</sub></b>	Voltage that provides Maximum Power
<b>P̄</b>	Average Deposition Power
<b>P<sub>m</sub></b>	Maximum Power Provided by DSSC
<b>P<sub>in</sub></b>	Input Light Source's Power
<b>n<sub>0</sub></b>	Raman Laser Frequency